2012

Monitoring thermal fatigue damage in nuclear power plant materials using acoustic emission

R. M. Meyer, *Pacific Northwest National Laboratory*
P. Ramuhalli, *Pacific Northwest National Laboratory*
B. E. Watson, *Pacific Northwest National Laboratory*
S. G. Pitman, *Pacific Northwest National Laboratory*
T. J. Roosendaal, *Pacific Northwest National Laboratory*, et al.

Monitoring thermal fatigue damage in nuclear power plant materials using acoustic emission

R. M. Meyer*, P. Ramuhalli, B. E. Watson, S. G. Pitman, T. J. Roosendaal, L. J. Bond
Pacific Northwest National Laboratory, 902 Battelle Boulevard, Richland, WA, USA 99352

ABSTRACT

Proactive aging management of nuclear power plant passive components requires technologies to enable monitoring and accurate quantification of material condition at early stages of degradation (i.e., pre-macrocrack). Acoustic emission (AE) is well-suited to continuous monitoring of component degradation and is proposed as a method to monitor degradation during accelerated thermal fatigue tests. A key consideration is the ability to separate degradation responses from external sources such as water spray induced during thermal fatigue testing. Water spray provides a significant background of acoustic signals, which can overwhelm AE signals caused by degradation. Analysis of AE signal frequency and energy is proposed in this work as a means for separating degradation signals from background sources. Encouraging results were obtained by applying both frequency and energy filters to preliminary data. The analysis of signals filtered using frequency and energy provides signatures exhibiting several characteristics that are consistent with degradation accumulation in materials. Future work is planned to enable verification of the efficacy of AE for thermal fatigue crack initiation detection. While the emphasis has been placed on the use of AE for crack initiation detection during accelerated aging tests, this work also has implications with respect to the use of AE as a primary tool for early degradation monitoring in nuclear power plant materials. The development of NDE tools for characterization of aging in materials can also benefit from the use of a technology such as AE which can continuously monitor and detect crack initiation during accelerated aging tests.

Keywords: Acoustic emission, thermal fatigue, early degradation, on-line monitoring, nondestructive examination, nuclear power plants

1. INTRODUCTION

Identification of early degradation (pre-macrocrack) for passive nuclear power plant (NPP) components (e.g., pipes, pressure vessel, etc.) is necessary to support the development of proactive aging management approaches.[1, 2] Early degradation is manifest as changes or phenomena at the grain and grain-boundary microstructural level including dislocation generation and motion, void formation, phase precipitation, changes to grain size or orientation, etc.[3] Either individually or in small numbers, such phenomena are generally not detectable using conventional NDE technologies that interrogate relatively large volumes of material. However, when occurring (and averaged) over significant volumes, these phenomena can be observed using some NDE technologies through their influence on underlying bulk material properties (e.g., elastic, electromagnetic, thermal, etc.).[1, 3] Some of the most promising techniques for early degradation monitoring include those based on micro-magnetic[3, 4] and non-linear ultrasonic measurements,[5] and it is anticipated that other suitable techniques will be developed as the field of research continues to mature. When there is interest in determination of remaining useful life (RUL) prediction, it is also necessary to identify signatures in NDE signals that accurately correlate with and reflect material condition and that can be tracked from early stages of damage through to failure. Efforts to develop algorithms for the extraction and tracking of such parameters for a set of micro-magnetic and non-linear acoustic measurements have been demonstrated and reported.[6, 7]

Correlation of NDE measurements to localization, degradation initiation, and small crack phenomena is essential to the development of early degradation monitoring tools. Variability in the initial morphology and condition, particularly surface condition of specimens, can result in significantly different lifetimes for specimens when subject to similar aging conditions, making it difficult to anticipate initiation and then remaining life simply based on aging stressor parameters (e.g., number of cycles). In seeking to understand and quantify degradation and aging, many of the technologies under investigation for early degradation applications are applied to samples periodically and crack initiation is often detected through visual observations. In relying on visual observation, it is possible that failure is not detected until degradation

* ryan.meyer@pnl.gov; phone 1 509 372-4753; fax 1 509 372-4753; www.pnl.gov

Nondestructive Characterization for Composite Materials, Aerospace Engineering, Civil Infrastructure, and Homeland Security 2012, edited by Andrew L. Gyekenyesi, Tzu-Yang Yu, Peter J. Shull, Aaron A. Diaz, H. Felix Wu,
Proc. of SPIE Vol. 8347, 83470D · © 2012 SPIE · CCC code: 0277-786X/12/$18 · doi: 10.1117/12.915458

has progressed significantly beyond initiation. Acoustic emission (AE) can significantly benefit early degradation studies through providing a means to continuously monitor for signs of crack initiation. AE can potentially allow more consistent detection of crack initiation by alerting investigators to changes in material condition that are characteristic of crack initiation as soon as these changes begin to occur. This interest extends beyond laboratory investigations of early degradation using AE, and extends to field applications of AE for condition monitoring.

Thermal fatigue is one damage mechanism that poses a threat to extended operation of NPPs, and is therefore a candidate degradation mechanism on which to base the development and testing of tools for monitoring early stages of damage.[8] Thermal fatigue can be caused by thermal stratification or mixing of reactor coolant water. At the point of mixing, flow is turbulent in nature, subjecting the adjacent pressure boundary to cyclic temperature fluctuations as a consequence of turbulent mixing. These temperature fluctuations induce thermal stresses in pressure boundary components that can eventually lead to crack initiation and growth. Thermal fatigue cracks can be induced in both base metal and weld metal materials.[9, 10] Thermal fatigue is studied in laboratory environments under accelerated conditions using an apparatus to rapidly heat and cool specimens. Cooling is often achieved by flowing water or air over the surface of the heated material.[9, 10]

In this paper, methods are proposed for the detection and monitoring of early degradation in materials with AE by analyzing signals with respect to frequency and energy. In the apparatus employed to fatigue samples, a water spray is used to cool specimens. This introduces a significant source of acoustic signals external to the specimen. The timing and location of noise from the water spray is expected to generally coincide with signals from crack formation and propagation. A significant challenge, then, is detecting evidence of degradation among the significant background of signals introduced by water spray. Section 2 provides background information supporting this approach. Section 3 describes the thermal fatigue specimens, the thermal fatigue apparatus, and associated AE monitoring system with initial results presented in Section 4. Discussions of these results are provided in Section 5 and concluding remarks are given in Section 6.

2. BACKGROUND

Post-processing and analysis of the frequency and energy of AE signals is employed in this work in an effort to separate AE signals associated with degradation from AE signals generated by external sources. This approach is justified given an understanding of how thermal fatigue evolves to failure, and knowledge gained from prior field and laboratory experience using AE to detect and monitor the growth of cracks in metal components.

2.1 Evolution of thermal fatigue damage

Thermal fatigue damage of materials can lead to cracking as a result of stress accumulation caused by thermal expansion and contraction in a constrained media. In a component made from completely homogenous material, macroscopic stresses can build up in the component as a result of thermal expansion if the boundaries of the component are constrained. In duplex stainless steels, microscopic stresses arise between different phases as a consequence of mismatch in the thermal expansion coefficients of each phase. In 304 stainless steel, the α-ferrite phase (bcc) and γ-austenite (fcc) phase are coexisting, resulting in a complex distribution of stresses caused by thermal fatigue. Pure thermal loading often results in the greatest amount of stress being distributed at the surface of the component with the stress concentration decreasing towards the interior. Continued thermal cycling can lead to the accumulation of localized stress at sites throughout the material, eventually leading to stress relaxation through the formation of cracks. The process is analogous to failure by mechanical fatigue. Fatigue failure is commonly divided into crack initiation, propagation, and failure stages. During propagation, growth of the crack continues at a steady rate determined by the magnitude of the stress intensity factor at the tip of the crack. Once the crack reaches a critical size, the component is weakened sufficiently to undergo gross fracture in response to external loading conditions. Thermal fatigue often induces a network of shallow cracks distributed over a given area; however, individual thermal fatigue cracks can grow larger to form dominant cracks.[9]

2.2 Experience gained from AE field testing for flaw growth monitoring in the nuclear industry

The U.S. Nuclear Regulatory Commission (NRC) sponsored a significant effort to understand the viability of AE for monitoring of flaws in NPP components.[11] This work involved demonstrations on intermediate-sized pressure vessels and on actual field units at Watts Bar Unit 1[12] and Limerick Unit 1.[13] Determinations of background noise caused by coolant flow showed that it was most significant at low frequencies (below 200 kHz) and decreased significantly at

higher frequencies. The investigators reported that signals associated with cracking had frequency components that were generally greater than what was observed in coolant noise and used this as a basis for developing AE sensors that were resonant in the 400 kHz–600 kHz range. This allowed reliable detection of AE signals from growing flaws even with a large background of AE signals provided by flowing coolant. Hutton and colleagues[11] successfully employed metal waveguides during field demonstrations to help isolate sensitive piezoelectric sensors from high coolant temperatures. The waveguides were determined to have an attenuation constant of approximately 1.5 dB/m.

2.3 Recent laboratory tests on large-scale components

Recently, AE was employed with guided ultrasonic waves (GUW) to monitor the evolution of mechanical fatigue damage in a Schedule 80 (10.16-cm; 4-inch diameter) 304 stainless steel pipe specimen. The pipe was subjected to cyclic loading using the four-point bend method. Using Physical Acoustic Corporation model R15α sensors, signals associated with crack initiation and propagation were observed to have frequency centroids between 200 kHz and 230 kHz. Signals associated with cracking also had very short duration (< 200 μs) and amplitudes less than 55 dB.[14]

Recently, AE has been applied to monitor the simulated failure of the main cooling pipe of a nuclear power plant.[15] In this case, the pipe specimen underwent cyclic hydraulic loading. The amplitude and energy of AE events were considered for indications of failure, and the amplitude distribution and event rate were correlated to damage stage. In this case, amplitude and energy of observed signals increased in latter stages of component lifetime and event rate exhibited an increase with lifetime as well.

3. EXPERIMENTAL SETUP

Tubular specimens (Figure 1) were selected for these bench-scale investigations of thermal fatigue. The specimens are fabricated from 304 stainless steel and approximately 500-mm long with an outside diameter (OD) of 25.4 mm (1 inch) and a wall thickness of 6.25 mm (0.246 inch). The tubular specimens were heated from the inside with periodic cooling on the outside. Heating was accomplished by means of a cartridge heater on the inside of the hollow specimen (Figure 1), while cooling was performed using water spray from the OD. The resulting thermal stresses initiate a crack (thermal fatigue crack) on the outside surface of the hollow specimen, providing easy access for NDE measurements as well as planned destructive analysis of the specimens.

Figure 1. Photograph of cartridge heater (top) and tubular 304 stainless steel specimens (bottom) used in this study.

Two test stations were set up for this study (Figure 2). At each station, one specimen was heated to temperatures up to 600°C and cooled to ambient temperatures by a periodic water spray controlled by a timed solenoid valve arrangement. Figure 3 presents a snapshot of the fatigue process in operation at both stations, with one specimen (upper) just starting the heating portion of a cycle while the other specimen (bottom) is just starting the cooling portion of a cycle. Thermocouples (type K) were used to monitor the heating and cooling cycles. The thermal cycles had a period of approximately 50 seconds, or 72 cycles per hour. Specimen heating consumed 46 seconds of the cycle while 4 seconds were consumed during cooling. The temperature was cycled from near ambient up to 600°C. These settings caused a thermal fatigue crack to initiate approximately between 8,000 to 10,000 cycles.

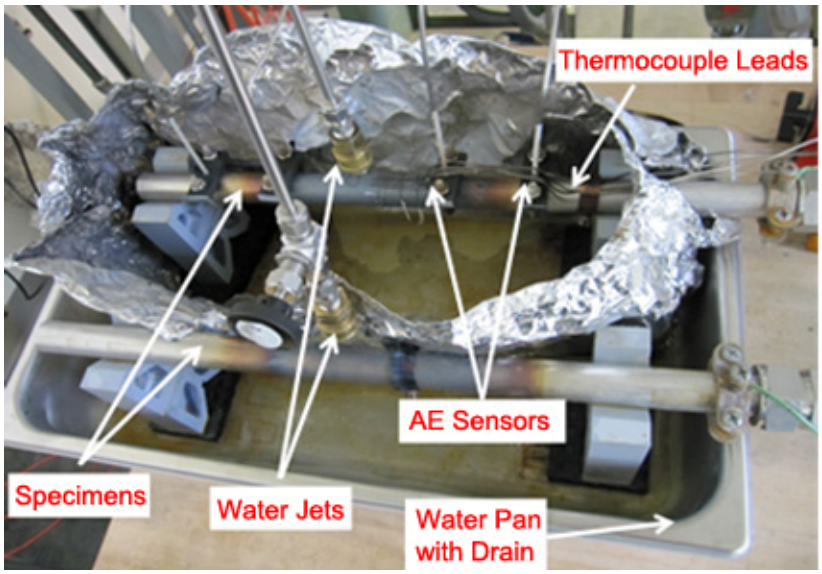

Figure 2. Photograph of test stations for performing thermal fatigue cycling of specimens with labels indicating positions of the water jets, specimens, thermocouple leads, and AE sensors.

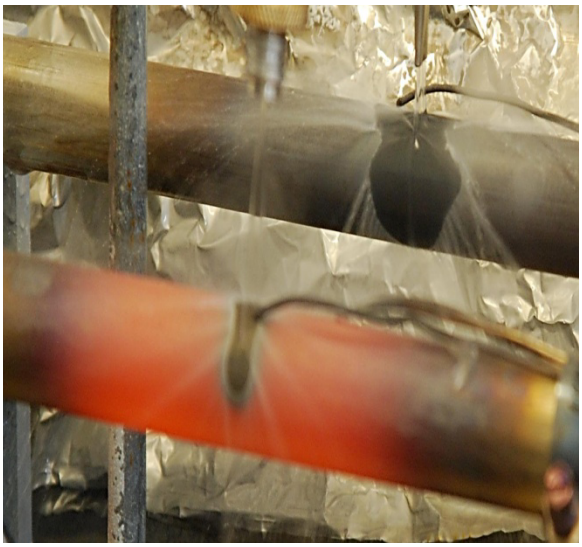

Figure 3. Snapshot of the thermal fatigue process in operation at both stations, with one specimen (upper) just starting the heating cycle while the other specimen (bottom) is just starting the cooling cycle.

The thermal fatigue specimens were instrumented with a linear array of AE transducers each coupled to the specimen through waveguides to protect and isolate the transducers from the temperature at the surface of the specimen. Figure 4 shows the four R15α transducers (Physical Acoustics Corporation - PAC) with resonant frequencies near 150 kHz attached along the length of the specimen. The waveguides consisted of cylindrical stainless steel rods approximately 60 cm (24 inches) in length with a diameter of 3.2 mm (0.125 inch). An eight-channel digital acoustic emission system, model μDISP, was employed to record and process AE signals. Interfacing with the system was conducted through the AEWin software located on a laptop computer. The μDISP AE processor allows for input of external parametric signals. Temperature cycles were recorded by the AE system to assist in data analysis. A sample plot of recorded temperature cycles is included in Figure 5.

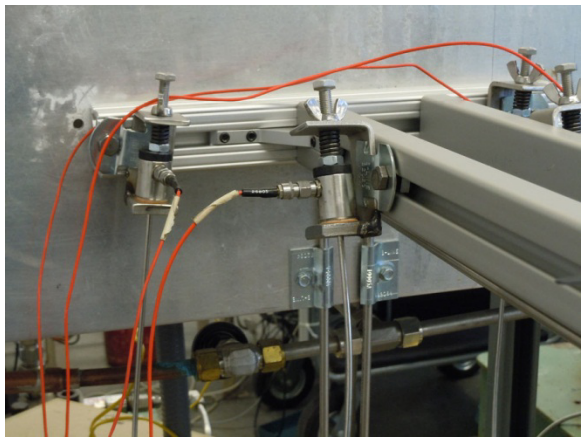

Figure 4. Photograph of AE sensor mounting and interface with stainless steel waveguides.

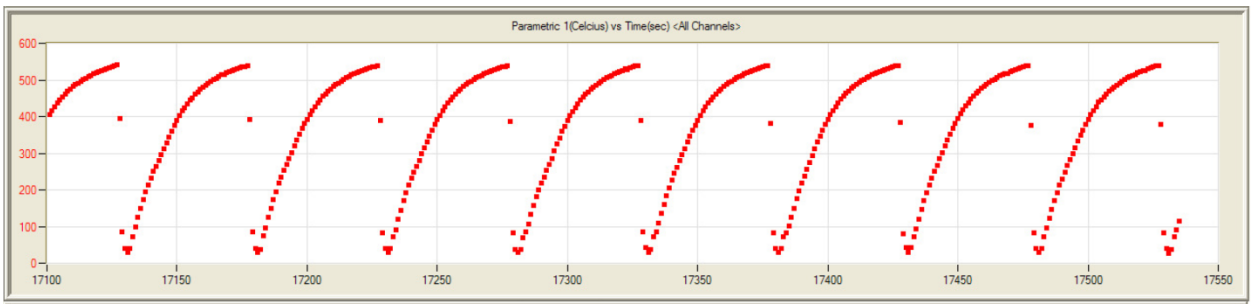

Figure 5. Sample of temperature data collected using the digital AE system to aid in analysis of AE signals.

4. RESULTS

Preliminary data was collected on a single specimen thermally cycled until cracking was observed visually (near 8000 cycles). The purpose of cycling the specimen was partly to optimize the AE system setup. A rearrangement of the waveguides was conducted at 2670 cycles, and the data prior to this rearrangement is not included here. The specimen was thermally fatigued over a series of intervals between which the cycling was paused to allow for other NDE measurements and to check the integrity of the interfaces between the AE sensor and specimen. Following the seventh interval, the AE system "froze" and failed to collect data during 600 thermal cycles. The AE system was restarted at the beginning of the next interval, which is referred to as interval 8, and performed satisfactorily until failure was observed during interval 10. A brief summary of the cycling intervals and AE data is provided in Table 1.

In an initial effort to discriminate degradation signals from signals caused by external sources, signals were sorted based on centroid frequency by specifying a cutoff centroid frequency of 190 kHz. Signals with centroid frequencies greater than this cutoff were attributed to degradation and retained, while signals below this cutoff were attributed to the background contributed by external sources and eliminated. The energy spectrum of background signals is provided in Figure 6 a) and the AE activity associated with the background is provided in Figure 6 b) for the thermal fatigue intervals in Table 1. The AE activity is represented as hits per cycle and cumulative hits throughout the monitored lifetime of the specimen. Figures 7 a) and 7 b) show cyclic temperature variation and AE activity over six cycles during interval 1 and 9. Of significant interest in these figures is the change in the shape of the thermocouple signal between interval 1 and 9. The waveform observed for interval 9 is representative for what was observed during interval 5 through 10 and was likely caused by trapping of water on the surface of the specimen after replacing a failed thermocouple at the beginning of interval 5. The trapped water required several seconds to boil off, thus impacting the thermocouple signal as shown. The energy spectrum for signals with centroid frequency greater than 190 kHz is provided in Figure 7 c) and the AE activity for these signals is provided in Figure 7 d).

Table 1. Summary of AE data collected over several thermal fatigue intervals spanning all but the earliest stages of a specimen's lifetime. Interval 5 is shaded green to highlight thermocouple failure and replacement at the beginning of the interval. No AE data was collected between intervals 7 and 8 (highlighted light blue), and cracking was visually observed during interval 10 (orange highlight).

Interval	Cycles	Cumulative Cycles	Total Hits	Total Energy (aJ)	Hits/Cycle	Energy/Hit (aJ)
1	486	3156	141223	5.50E+10	290	3.89E+05
2	522	3678	219286	7.00E+10	420	3.19E+05
3	498	4176	94648	3.50E+10	190	3.70E+05
4	1200	5376	269136	1.10E+11	224	4.09E+05
5	222	5598	52313	1.85E+10	235	3.54E+05
6	210	5808	39613	1.40E+10	188	3.53E+05
7	90	5898	14144	1.40E+10	157	9.90E+05
---	600	6498	---	---	---	---
8	396	6894	75010	7.80E+10	189	1.04E+06
9	1122	8016	256917	2.25E+11	228	8.76E+05
10	306	8322	64446	4.80E+10	210	7.45E+05

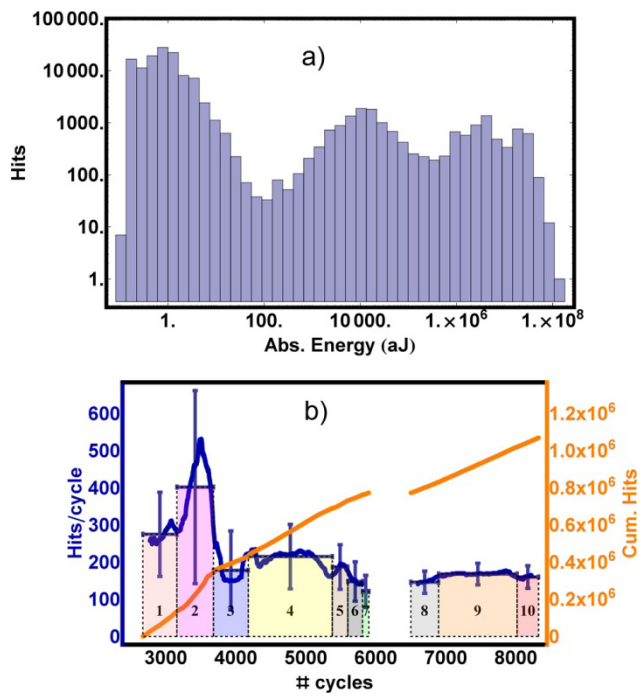

Figure 6. a) Energy spectrum of background signals (< 190 kHz) collected during interval 1, and b) background AE activity versus component lifetime represented as hits/cycle and cumulative hits.

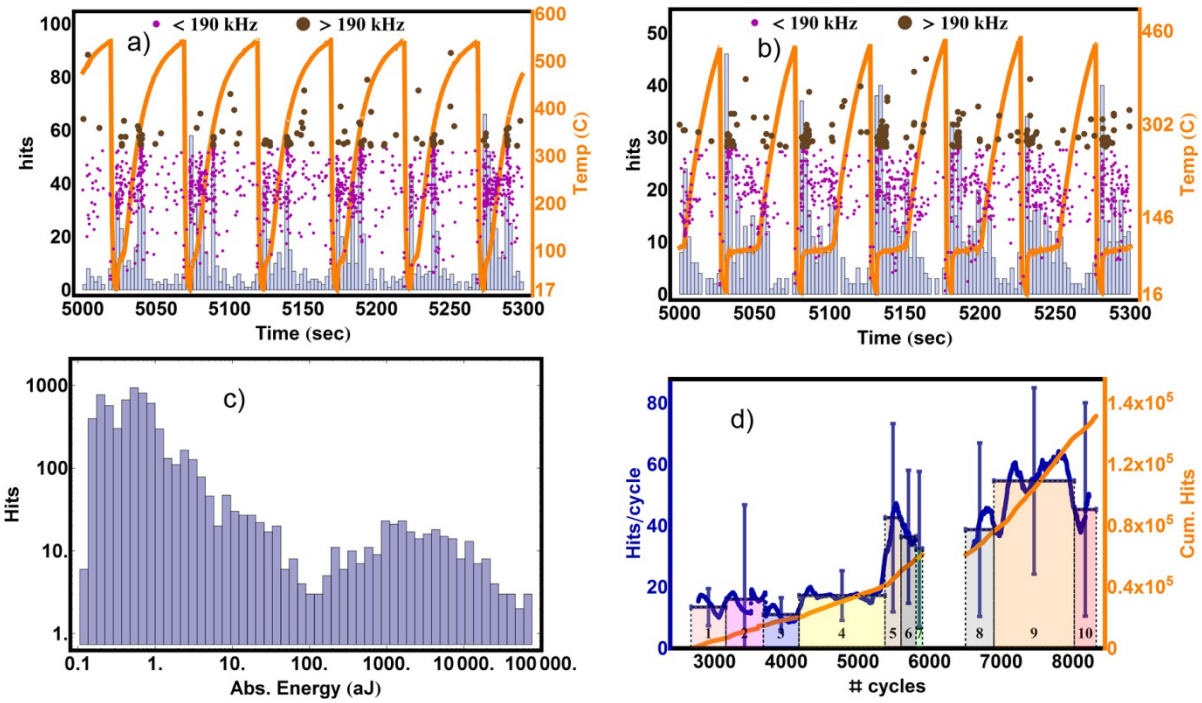

Figure 7. a) AE activity collected over six thermal cycles during interval 1 along with a plot of the thermocouple signal during these cycles; signals with centroid frequency greater than 190 kHz are highlighted using enlarged dots. b) AE activity collected over six thermal cycles during interval 9 along with a plot of the thermocouple signal during these cycles. c) the energy spectrum obtained for signals in interval 1 with a centroid frequency greater than 190 kHz. d) the activity of AE signals with centroid frequency greater than 190 kHz over the lifetime of the specimen.

Next, an energy-based filter was cascaded with the frequency-based filter in an effort to further discriminate external sources of AE. The energy spectrum of signals with centroid frequency greater than 190 kHz is provided in Figure 8 a) for intervals 1 and 10 (labeled as "3000 cycles" and "8000 cycles," respectively). Figure 8 a) indicates significant overlap between the two spectrums with some exceptions, the most significant of which occurs over the energy range of approximately 1–100 aJ with interval 10 exhibiting a much greater number of hits in this energy range than interval 1. AE activity over six cycles during interval 9 is plotted along with the thermocouple signal and displayed in Figure 8 b). Also in Figure 8 b) is a plot of when hits both above and below 190 kHz occur within these cycles, with hits above 190 kHz also subject to the energy window. Finally, with both centroid frequency and energy filters applied, AE activity in hits/cycle and cumulative hits is plotted from interval 1 to interval 10 in Figure 8 c).

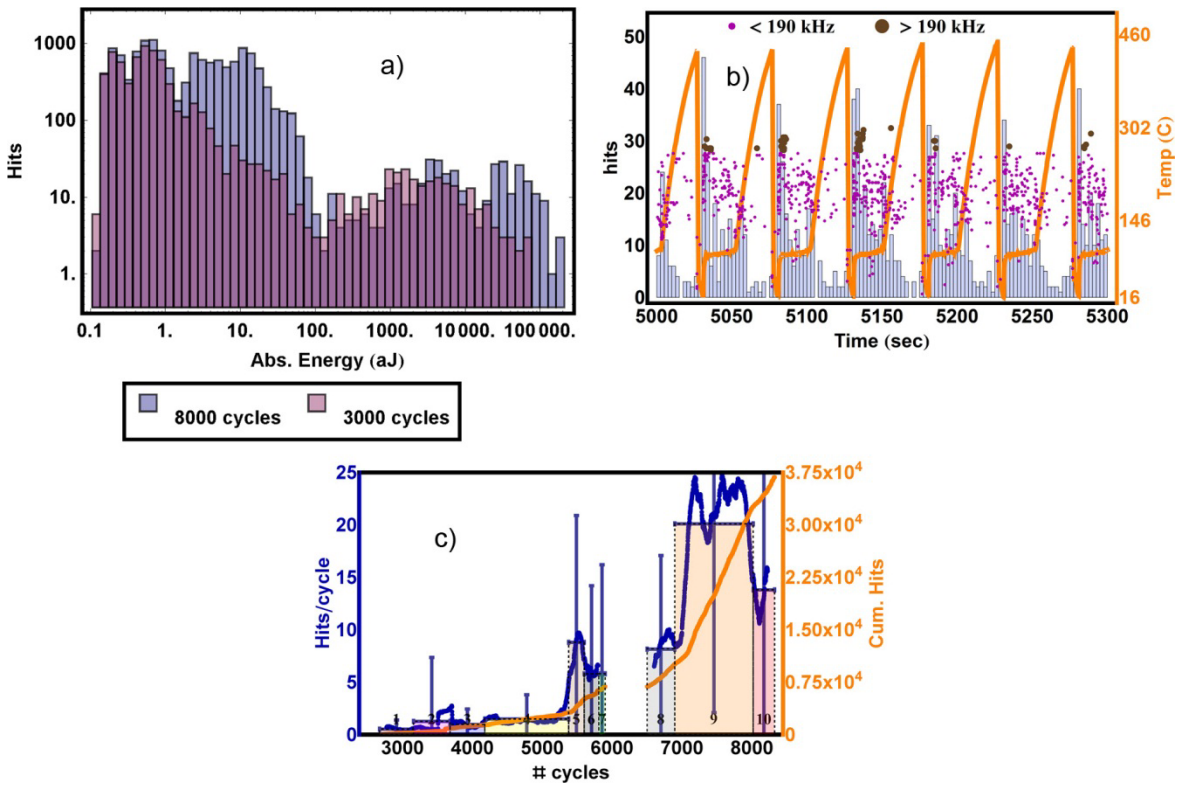

Figure 8. a) Overlapping energy spectra for high frequency signals (centroid frequency > 190 kHz) during interval 1 and interval 10, respectively (labeled as "3000 cycles" and "8000 cycles," respectively (areas of pink bars "3000 cycles" that overlap blue bars "8000 cycles" are represented as magenta); b) AE activity observed over six thermal cycles during interval 9, including a simultaneous plot of the thermocouple signal; and c) the activity of AE signals filtered over centroid frequency (> 190 kHz) and energy (5–100 aJ) over the lifetime of the specimen.

5. DISCUSSION

The trend observed in Figure 8 c) is encouraging and agrees with early damage evolution through the accumulation of material inhomogeneities. The large standard deviations observed are consistent with discontinuous or "burst-like" emissions that are often associated with certain forms of degradation such as cracking or decohesion and rupture of precipitates or inclusions.[16] In Figure 7 d) the observed trend still exhibits general behavior in line with expectations from damage accumulation but the trend is much weaker and indicates that signal analysis based only on the centroid frequency parameter may be insufficient for discrimination of damage signals from signals originating from the external sources. Given the results observed in Figure 8 c), it is important to interpret the data with respect to material condition. Specifically, there is a need to conclusively determine if there are any features in the AE data that are indicators of crack initiation, and if the stage of degradation can be inferred from AE behavior. The data evaluated in this limited study is insufficient to make conclusive determinations. True-state measurements are required to determine whether AE behavior can be applied to estimate the degradation state. Further, analysis of the response of several specimens is needed so that conclusions regarding the interpretation of AE behavior can be made with high confidence. Both of these steps are planned in future efforts.

Additional refinements to the system are planned as well. As mentioned above, replacement of a thermocouple at the beginning of interval 5 resulted in trapping water on the surface of specimens and subsequent boiling. This boiling introduced a source of AE signals for intervals 5–10 that was not present in intervals 1–4. The amount of influence this has on observed trends in the AE data is not known. The thermocouple replacement is coincident with the observation of a significant increase in AE activity in Figures 7 d) and 8 c). On the other-hand, significant increases in AE activity are observed during later intervals that appear to be independent of thermocouple repositioning. In addition, the relative increase in acoustic noise after thermocouple replacement due to boiling is not known. The data in Figure 8 b) indicates that signals included in Figure 8 c) are consistently emitted just after the cooling period and appear clustered in only a

brief moment during the entire thermal cycle, whereas boiling is clearly present over a much larger portion of the thermal cycle. This AE behavior is consistent with expectations of signals emitted by degradation, which would occur at moments of greatest stress concentration during the thermal cycle. It is still possible that the observed signals are associated with only a certain stage of boiling, such as nucleate boiling; therefore, boiling cannot be ruled out as a potential source for these signals.

In addition to boiling, the relative positioning of specimens and the water spray could influence AE response over specimen lifetime if the relative positioning is shifted. The uncertainties caused by boiling and relative positioning of water spray and specimen can be minimized. This will be the focus of planned refinements to the system. Other refinements will focus on minimizing sources of fretting and potentially using wide-band transducers.

6. CONCLUSIONS

Advanced signal analysis capabilities offered by digital AE systems can benefit the development of tools to monitor early degradation behavior in NPP materials. In accelerated thermal fatigue aging studies, a significant background of AE signals is introduced by water sprays used for specimen cooling. Analysis of signal frequency and energy is proposed as a method for discriminating sources of degradation from external sources such as water spray. This analysis was performed on AE data collected from a single thermal fatigue specimen that was cycled to failure, generating encouraging results. To enable more definitive conclusions, plans for future work include refining the thermal fatigue apparatus, correlating AE results with true-state, and assessing data obtained from multiple specimens. While the emphasis has been placed on the use of AE for crack initiation detection during accelerated aging tests, this work also has implications with respect to the use of AE as a primary tool for early degradation monitoring in NPP materials.

ACKNOWLEDGEMENTS

Support for this work from the U.S. Department of Energy (DOE–NE) Light Water Reactor Sustainability (LWRS) program is gratefully acknowledged. This work was conducted at Pacific Northwest National Laboratory (PNNL), which is operated by Battelle on behalf of the U.S. Department of Energy.

REFERENCES

[1] Bond, L. J., Doctor, S. R., Griffin, J. W. *et al.*, “Damage assessment technologies for prognostics and proactive management of materials degradation (PMMD),” Nucl. Tech. 173, 46-55 (2011).

[2] Bond, L. J., “Moving beyond nondestructive examination to proactive management of materials degradation,” J. Pres. Vessel Technol. 134(1), 014501-014508 (2012).

[3] Raj, B., Moorthy, V., Jayakumar, T. *et al.*, “Assessment of microstructures and mechanical behaviour of metallic materials through non-destructive characterisation,” Int. Mater. Rev. 48(5), 273-325 (2003).

[4] Dobmann, G., “NDE for material characterization of aging due to thermal embrittlement, fatigue and neutron degradation,” Int. J. Mater. Prod. Tech. 26, 122-139 (2006).

[5] Jhang, K.-Y., “Nonlinear ultrasonic techniques for non-destructive assessment of micro damage in material: A review,” Int. J. Precis. Eng. Manuf. 10(1), 123-135 (2009).

[6] Ramuhalli, P., Griffin, J. W., Fricke, J. *et al.*, "Diagnostics and prognostics tools for assessing remaining useful life of nuclear power plant materials." Enabling Sustainable Systems, Proceedings 2011 Society for Machinery Failure Prevention Technology Meeting (MFPT 2011), (2011).

[7] Ramuhalli, P., Bond, L. J., Griffin, J. W. *et al.*, "A bayesian prognostic algorithm for assessing remaining useful life of nuclear power components." 7th International Topical Meeting on Nuclear Plant Instrumentation, Control and Human Machine Interface Technologies (NPIC&HMIT 2010), 875-886 (2010).

[8] IAEA, [Advanced surveillance diagnostics, and prognostics techniques used for health monitoring of systems, structures, and components in nuclear power plants: CRP Report Volume I], IAEA-NE-D-NP-T-3.14, International Atomic Energy Agency (IAEA), Vienna, Austria (2012 (in press)).

[9] Kemppainen, M., [Realistic artificial flaws for NDE qualification – a novel manufacturing method based on thermal fatigue], Helsinki University of Technology, Espoo, Finland, http://lib.tkk.fi/Diss/2006/isbn9512282631/ and http://lib.tkk.fi/Diss/2006/isbn9512282631/isbn9512282631.pdf (2006).

[10] Virkkunen, I., [Thermal fatigue of austenitic and duplex stainless steels], Helsinki University of Technology, Espoo, Finland, http://lib.tkk.fi/Diss/2001/isbn9512256878/isbn9512256878.pdf (2001).
[11] Hutton, P. H., "Listening to reactor pressure boundaries for the sounds of cracks and leaks," Nucl. Eng. Int. 38(47), 38-40 (1993).
[12] Hutton, P. H., Dawson, J. F., Friesel, M. A. *et al.*, [Acoustic emission monitoring of hot functional testing: Watts Bar Unit 1 nuclear reactor], NUREG/CR-3693, U.S. Nuclear Regulatory Commission, Washington, D.C. (1984).
[13] Hutton, P. H., Friesel, M. A., and Dawson, J. F., [Continuous ae crack monitoring of a dissimilar metal weldment at Limerick Unit 1], NUREG/CR-5963, PNL-8844, U.S. Nuclear Regulatory Commission, Washington, DC (1993).
[14] Meyer, R. M., Cumblidge, S. E., Ramuhalli, P. *et al.*, "Acoustic emission and guided wave monitoring of fatigue crack growth on a full scale pipe specimen." Proceedings of SPIE, Volume 7984 - Health Monitoring of Structural and Biological Systems 2011; SPIE Smart Structures/NDE, (2011).
[15] Ai, Q., Liu, C.-X., Chen, X.-R. *et al.*, "Acoustic emission of fatigue crack in pressure pipe under cyclic pressure," Nucl. Eng. Des. 240(10), 3616-3620 (2010).
[16] Harris, D. O., and Dunegan, H. L., "Continuous monitoring of fatigue-crack growth by acoustic-emission techniques," Exp. Mech. 14(2), 71-81 (1974).